Supplemental Figure 1

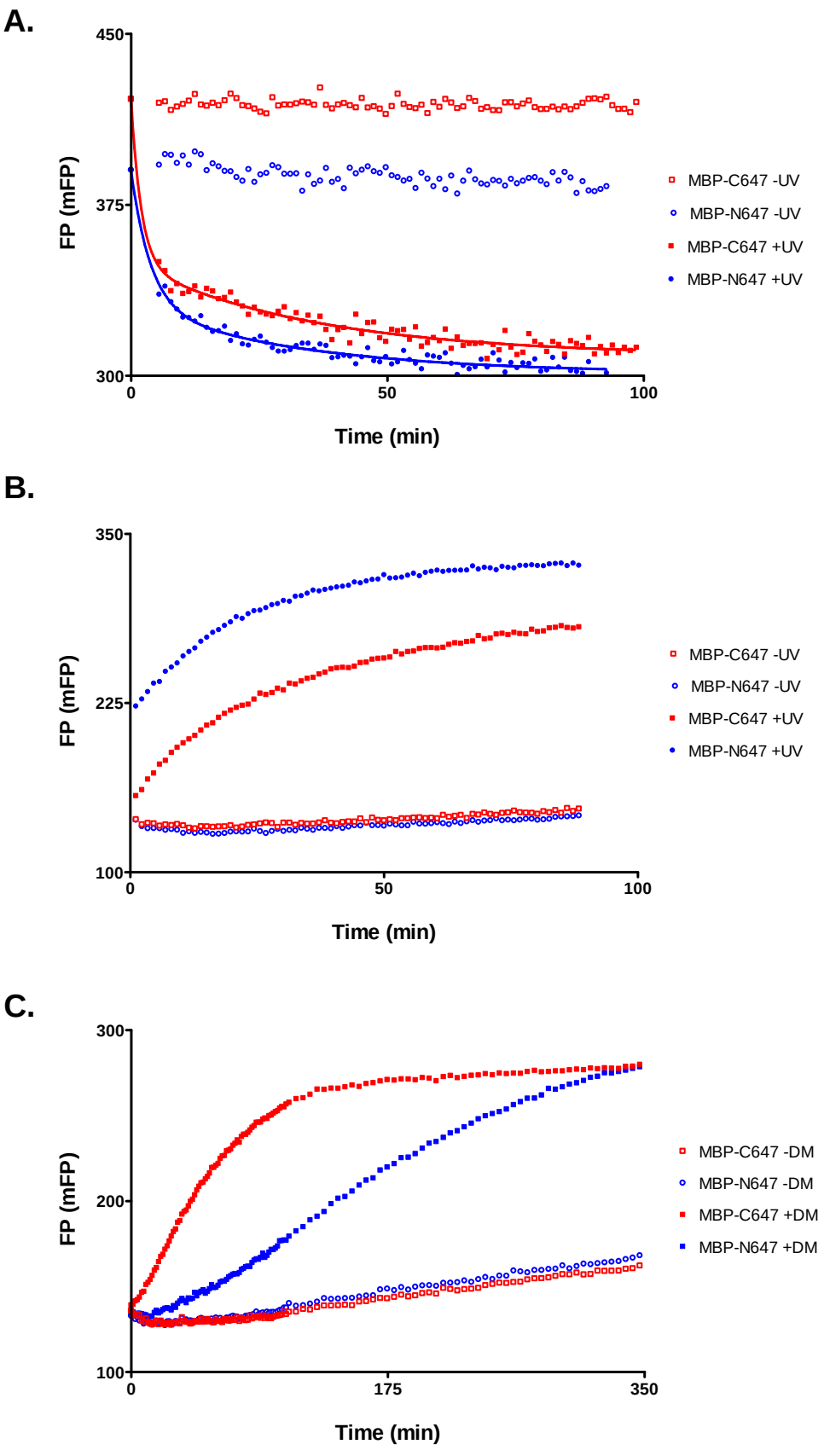

Supplemental Figure 1. *(*A) Monitoring dissociation of photocleavage products with an N-terminal or C-terminal Alexa647 fluorescent group on the photocleavable peptides **MBP-C647** and **MBP-N647**. (B) Association of **MBP-488** was followed in the 488nm channel. Open symbols represent complexes without UV irradiation (□ = **MBP-C647**, ○ = **MBP-N647**), closed symbols complexes with UV irradiation (■ = **MBP-C647**, ● = **MBP-N647**). The **MBP-488** association phase following cleavage of **MBP-N647** mirrored the early rapid dissociation kinetics of the N-terminal **N647** fragment (A). A higher FP reading was observed following cleavage of DR2 loaded with **MBP-N647**, due to more efficient photocleavage of this peptide. (C) Effect of DM on displacing **MBP-N647** or **MBP-C647**, monitored by binding of **MBP-488**. DM accelerated exchange of the **MBP-N647** and **MBP-C647** peptides by **MBP-488**, but the N-terminal Alexa647 group in the **MBP-N647** peptide reduced the activity of DM on this complex compared to the **MBP-C647** peptide, consistent with mutagenesis data that mapped the DM binding site close to the peptide N-terminus (Doebele et al., 2000).

Supplemental Table 1: Yield of DR2-peptide complexes and affinity of peptides for DR2

	MBP_{85-99}	**MBP-P1***	**MBP-P2***	**MBP-P3***	**MBP-P4***	**MBP-P5***
Yield complex†	~300 μg	~3 μg	~30 μg	~30 μg	~300 μg	~50 μg
Affinity difference‡	1	306	52	355	3	11

† Recovery after all purification steps
‡ Fold difference affinity for DR2 compared to index $MBP_{85–99}$

SUPPLEMENTAL EXPERIMENTAL PROCEDURES

Peptide Synthesis

Standard Fmoc-based solid-phase peptide chemistry was employed for the synthesis of peptides **MBP-P1*** - **MBP-P5***. N-terminal capping was accomplished by coupling of a 4-aminobutyric acid succinimide ester endowed with a dinitrophenyl (Dnp) moiety. Cleavage from the resin and concomitant removal of the side-chain protecting groups was followed by HPLC purification and lyophilization of the final products. LC/MS analysis and MALDI TOF MS confirmed the identity and homogeneity of the peptides.
Purified peptides of the sequence Dnp-C(SStBu)NPVVHF-Anp-KNIVTPC were labeled with thiol-reactive maleimide derivatives of AlexaFluor647 C_2-maleimide (Invitrogen, Carlsbad, CA). The attachment of the fluorecent probe to the C-terminal cysteine was accomplished using a modified procedure of the manufacturer's instructions. Typically, in an eppendorf tube, shielded from light with alumium foil, 77 μL of a stock solution of peptide Dnp-C(SStBu)NPVVHF-Anp-KNIVTPC in N,N-dimethylformamide (10 mM) was diluted with 77 μL water and 30 μL phosphate buffer (1 M, pH 7) after which a stock solution of AlexaFluor647 C_2-maleimide in water (10 mM) was added. The reaction was allowed to proceed overnight with gentle shaking. LC/MS analysis confirmed quantative consumption of the starting material. The crude mixture was then purified by HPLC. Fractions containing the desired product were pooled and solvents evaporated *in vacuo*. Lyophilization of the final product afforded 1.1 mg, 0.35 μmol of **MBP-N647**.

The N-terminal derivitization with the AlexaFluor647 C_2-maleimide (Invitrogen, Carlsbad, CA) required initial blocking of the C-terminal free thiol, followed by release of thio-*tert*-Butyl protecting group under the agency of tributylphosphine. Therefore, to 65 μL of peptide stock Dnp-C(SStBu)NPVVHF-Anp-KNIVTPC (10 mM in DMF) was added 65 μL water and 7 μL phosphate buffer (1 M, pH 7) as well as 3.25 μL of N-ethylmaleimide (1M in DMF). After shaking for 2 hours, the reaction was quenched by the addition of 4.9 μL of 2-mercaptoethanol (1M in DMF) which was allowed to react for an additional hour. Having exposed the N-terminal free thiol, the peptide was HPLC purified and reacted with AlexaFluor647 C_2-maleimide (Invitrogen, Carlsbad, CA) as described above to furnish 1.0 mg, 0.32 μmol of the final product **MBP-C647**.

Modeling Methods

Each of the three models discussed in the main text were fit to the experimental data using a nonlinear regression package in MATLAB. All of the experiments used for parameter estimation involved the addition of **MBP-488** after 10 minutes of UV exposure to a well containing *e*MHC with or without DM. The relevant ordinary differential equations were solved to determine the concentrations of all species as a function of time and the concentration of *fp*MHC was plotted with the experimental data. In the analyses, the concentration of **MBP-488** was set to 0 nM for the first 10 minutes. After 10 minutes, the concentration was set to 200 nM to simulate the addition of **MBP-488** after the UV exposure. A good initial estimate for the unknown parameters was necessary to

get the regression package to converge on a reasonable solution. To obtain a good initial estimate, the unknown parameters were varied manually until the predicted *fp*MHC trajectory overlapped considerably with the experimental data. The nonlinear regression package was then used to refine the parameter estimates.

All reactions were assumed to be elementary, which means that reactions involving one species are first order, two species are second order, etc. A list of all of the possible reactions in the three proposed models in the main text is shown in **Supplemental Table 2**, along with the corresponding rate expressions. Reaction 2 was assumed to be irreversible because peptide removal to form *e*MHC is slow in the absence of UV and DM. Reactions 7 and 8 involve the UV cleavage of the peptide and the subsequent dissociation of the peptide fragments from DR2, respectively. These two events are assumed to be first order and fast. Reaction 9 is written in a completely general manner using the aggregation number, N, since the number of *e*MHC molecules involved in the reaction is unknown. In the event that the aggregation number is 1, this reaction represents the reversible unfolding of *e*MHC to an unreactive form. If the aggregation number is greater than 1, then this reaction represents the reversible aggregation of N *e*MHC molecules. All rates are written on a concentration basis, with concentrations in nM.

Supplementary Table 2: List of possible reactions and corresponding rate expressions

Index	Reaction	Rate Expression
2	$eMHC+MBP\text{-}488 \rightarrow fpMHC$	$r_2=k_2[eMHC][MBP\text{-}488]$
5	$DM\text{-}eMHC+MBP\text{-}488 \leftrightarrow fpMHC$	$r_5=k_5[DM\text{-}eMHC][MBP\text{-}488]-k_{-5}[DM][fpMHC]$
7	$pMHC \rightarrow p^*MHC$	$r_7=k_7[pMHC]$
8	$p^*MHC \rightarrow eMHC$	$r_8=k_8[p^*MHC]$
9	$N\ eMHC \leftrightarrow iMHC$	$r_9=k_9[eMHC]^N-k_{-9}N[iMHC]$
10	$eMHC+DM \leftrightarrow DM\text{-}eMHC$	$r_{10}=k_{10}[eMHC][DM]-k_{-10}[DM\text{-}eMHC]$

The set of equations corresponding to model 1 (Eq. 1) are given as

$$\frac{d}{dt}[pMHC] = -r_7 = -k_7[pMHC]$$
$$\frac{d}{dt}[p^*MHC] = r_7 - r_8 = k_7[pMHC] - k_8[p^*MHC]$$
$$\frac{d}{dt}[eMHC] = r_8 - r_2 = k_8[p^*MHC] - k_2[eMHC][MBP\text{-}488]$$
$$\frac{d}{dt}[fpMHC] = r_2 = k_2[eMHC][MBP\text{-}488]$$
$$[MBP\text{-}488]= [MBP\text{-}488]_0-[fpMHC] \qquad \text{(S1)}$$

where an algebraic species conservation relation is necessary in addition to the ordinary differential equations to calculate the concentration of **MBP-488** at each time point using species conservation. The values of both k_7 and k_8 were set to 1 min^{-1}, which allowed these reactions to go to completion during the 10 minute UV step as observed in experiments. No value of k_2 was able to capture the experimentally observed behavior at both short and long times.

The set of equations corresponding to model 2 (Eq. 2) are given as

$$\frac{d}{dt}[\text{pMHC}] = -r_7 = -\text{k}_7[\text{pMHC}]$$

$$\frac{d}{dt}[\text{p*MHC}] = r_7 - r_8 = \text{k}_7[\text{pMHC}] - \text{k}_8[\text{p*MHC}]$$

$$\frac{d}{dt}[\text{eMHC}] = r_8 - r_2 - r_9 = \text{k}_8[\text{p*MHC}] - \text{k}_2[\text{eMHC}][\text{MBP-488}] - (\text{k}_9[\text{eMHC}]^{\text{N}} \text{-k}_{\text{-9}}\text{N}[\text{iMHC}])$$

$$\frac{d}{dt}[\text{iMHC}] = r_9 = \text{k}_9[\text{eMHC}]^{\text{N}} \text{-k}_{\text{-9}}\text{N}[\text{iMHC}]$$

$$\frac{d}{dt}[\text{fpMHC}] = r_2 = \text{k}_2[\text{eMHC}][\text{MBP-488}]$$

$$[\text{MBP-488}] = [\text{MBP-488}]_0 \text{-}[\text{fpMHC}] \qquad \text{(S2)}$$

where an aggregation reaction has been added in order to account for the experimentally observed behavior at short and long times. This model has four parameters, in addition to k_7 and k_8 that were fit to the experimental data. A comparison of the model prediction and the experimental data for one set of parameters is shown in **Fig. 7B.**

The set of equations corresponding to model 3 (Eq. 3) are given as

$$\frac{d}{dt}[\text{pMHC}] = -r_7 = -\text{k}_7[\text{pMHC}]$$

$$\frac{d}{dt}[\text{p*MHC}] = r_7 - r_8 = \text{k}_7[\text{pMHC}] - \text{k}_8[\text{p*MHC}]$$

$$\frac{d}{dt}[\text{eMHC}] = r_8 - r_2 - r_9 - r_{10}$$

$$= \text{k}_8[\text{p*MHC}] - \text{k}_2[\text{eMHC}][\text{MBP-488}] - (\text{k}_9[\text{eMHC}]^{\text{N}} \text{-k}_{\text{-9}}\text{N}[\text{iMHC}]) - (\text{k}_{10}[\text{eMHC}][\text{DM}] \text{-k}_{\text{-10}}[\text{DM-eMHC}])$$

$$\frac{d}{dt}[\text{iMHC}] = r_9 = \text{k}_9[\text{eMHC}]^{\text{N}} \text{-k}_{\text{-9}}\text{N}[\text{iMHC}]$$

$$\frac{d}{dt}[\text{DM-eMHC}] = r_{10} - r_5$$

$$= \text{k}_{10}[\text{eMHC}][\text{DM}] \text{-k}_{\text{-10}}[\text{DM-eMHC}] - (\text{k}_5[\text{DM-eMHC}][\text{MBP-488}] \text{-k}_{\text{-5}}[\text{DM}][\text{fpMHC}])$$

$$\frac{d}{dt}[\text{fpMHC}] = r_2 + r_5$$

$$= \text{k}_2[\text{eMHC}][\text{MBP-488}] + (\text{k}_5[\text{DM-eMHC}][\text{MBP-488}] \text{-k}_{\text{-5}}[\text{DM}][\text{fpMHC}])$$

$$[\text{MBP-488}] = [\text{MBP-488}]_0 - [\text{fpMHC}]$$
$$[\text{DM}] = [\text{DM}]_0 - [\text{DM-eMHC}] \quad \text{(S3)}$$

where two additional algebraic species conservation relationships are necessary to calculate the concentrations of DM and **MBP-488** at all time points using species conservation. The values of the parameters obtained from model 2 (used to prepare the curve in **Fig. 7B)** were fixed and the additional parameters were fit to experiments where the amount of DM was varied. A comparison of the model predictions and the experimental data for one set of best-fit parameters is shown in **Fig. 7C**. Due to the large number of experiments, only a representative set of curves are shown in the figure. A summary of the quality of fit for all experiments can be found in **Supplemental Table 3.** The maximum and minimum percent deviations for each set of conditions were determined by first calculating the percent deviation of the model from the experimental data at all time points using the following equation

$$\%dev(t=\tau) = \frac{[fpMHC]_{predicted}(t=\tau) - [fpMHC]_{experimental}(t=\tau)}{[fpMHC]_{experimental}(t=\tau)} \quad \text{(S4)}$$

where *%dev* is the percent deviation and τ is a generic time value.

Supplementary Table 3: Quality of fit for all DM experiments used for parameter estimation. All quality of fit parameters have been calculated using data points collected within the first 100 minutes of each experiment. The largest magnitude of the percent deviation for all experiments occurred within the first two time points. Values of R2 are also reported to show that the overall quality of the fit is excellent for all sets of data as in Fig. 7C.

DM Concentration (nM)	R^2	Maximum % Deviation	Minimum % Deviation
0	0.956	18.91	0.14
150	0.988	24.52	0.20
300	0.995	12.66	0.03
500	0.979	61.55	0.03
1000	0.985	31.27	0.00
2000	0.976	24.61	0.01
5000	0.899	24.86	0.17

Parameter sensitivity

As indicated in the main text, we performed parameter sensitivity studies for all models, and found other sets of parameters that also fit the data well. The main mechanistic point derived from the kinetic analyses is that k_5 is greater than k_2, thereby indicating that DM-bound MHC is more peptide receptive than the receptive state of MHC alone. This result is robust to parameter sensitivity using model 3. As noted in the main text, it is also robust to other models that we explored which were designed such that lower values of k_5 might be able to fit the data. For example, we determined the smallest value of k_5 that

could predict the large initial slope observed in the experiments where DM was added. To obtain this smallest value, k_{-5} and k_{-10} were set to zero since reversible reactions would reduce the initial slope (requiring larger values of k_5). The value of k_{10} was set to a large value since this would create the largest concentration of DM-*e*MHC, which results in the smallest value of k_5 necessary to obtain the same rate. The initial slope of the data for 150 nM DM is the smallest in our experimental data set, and so fitting the initial slope of this data with this model would yield the smallest possible value of k_5. The initial slope could only be fit if k_5 was at least two times greater than k_2. So, even in such a model designed to obtain the smallest possible value of k_5, its value must be greater than k_2 in order to be in harmony with experimental data.